Driver Intervention Detection via Real-Time Transfer Function Estimation

Wouter S. Schinkel, Tom P. J. van der Sande, and Henk Nijmeijer, *Fellow, IEEE*

***Abstract*— Currently, the driver plays a crucial role in the safety of autonomous vehicles, functioning as the fall back for vehicle control systems. Fast and accurate detection of driver intervention is therefore of importance. In this article a novel driver intervention detection method for automated vehicles is presented and tested. Non-critical transitions are considered, excluding safety related applications. The transfer function between the electric power steering torque and steering column angle is estimated by perturbing the steering system with a known disturbance. This estimated value is used to detect whether a driver is intervening. The detection algorithm has been tested in simulations using a four degree-of-freedom vehicle model. The parameters of this vehicle model have been obtained via frequency response measurements performed on a test vehicle. Secondly, the performance of the algorithm has been tested with on-road measurements. The results show that driver intervention can be successfully detected within 0.4 seconds. The performance in terms of true and false detections has been analyzed, and the presented solution is shown to be robust to measurement noise and road disturbances.**

***Index Terms*— Autonomous vehicles, driver intervention, driver take-over, intelligent vehicles, vehicle measurements.**

I. Introduction

AUTOMATED vehicles can be classified from driving automation level 0 through 5 using the SAE J3016 standard [1]. Driving automation level 0 being fully manually operated vehicle and 5 being fully automated. Driving automation level 1 was realized in the 1990's with the implementation of adaptive cruise control, also known as ACC [2]. Level 3 and above is projected to be realized in the 2020's [3]. Driving automation level 3 requires the longitudinal and lateral vehicle motions to be controlled simultaneously in a specified operational design domain [1]. In vehicles up to level 3 the fallback for the vehicle control system is the driver. Because there is no automated fallback, the detection of driver intervention is a necessity. The driver may try to take over the control of the vehicle during a period of incertitude on the driver's part. However, for the vehicle to shift the control back to the driver, it must be able to detect the driver intervention.

A study on state-of-the-art solutions for driver intervention detection has revealed that additional hardware in the form of sensors and/or actuators is required for most solutions. The current solutions can be categorized as 1) vision systems, 2) biometric sensors, and 3) wearables and brought-in devices such as smartphones. An example of a vision system has been presented in [4]; a multi-view camera system observing the 3D movements of the driver's head and hands. This system is able to detect whether the driver is holding the steering wheel. The upper body motions are estimated in real-time using the hands and head movements. Another vision system has been presented in [5], where the authors implemented a convolution neural network based approach. In addition to detecting the number of hands on the steering wheel, this system is able to detect cellphone usage. According to the authors of [6], processing of visual data is mainly realized with machine learning and image processing techniques. In [7] the authors have presented a hand-tracking system using a depth sensor, which is claimed to be the first to achieve such a short response time in combination with the robustness and accuracy. This system is able to detect the number of hands on the steering wheel and make a distinction between touching and grabbing the steering wheel, all based on the position and shape of the hands and fingers. A driver state detection system using biometric sensors has been presented in [8], where combining a capacitive hand detection sensor with other physiological sensors allows for the determination of both touch and position of the driver's hands. The system is wireless and can therefore be placed in most vehicles as a retrofit. As an alternative, electrocardiograph signals can also be used to detect driver intervention. A driver recognition method which uses electrocardiograph signals from the hands has been presented in [9]. The add-on system is located on the steering wheel and is able to automatically adapt the vehicle settings based on the perceived driver. In [10], a wearable device named SafeWatch, developed to detect unsafe driving behavior, has been presented. From the estimated hand motions it can be determined whether a driver is holding the steering wheel. A similar approach has been presented in [11], where measurements from a wearable device (e.g., smart watch, fitness tracker) have been used. An accuracy of 99 % for the detection of hands on the steering wheel and 80 % for hands off has been achieved in experiments. The authors of [12] have used a similar type of device to determine the stress level of the driver by evaluating the steering behavior. In [13] an overview of novel methods, ongoing research, and trends for driver state and performance assessment has been presented. One of topics is the combination of in-vehicle information and brought-in sensors, such as smartphones. The authors of [6] have also presented an overview of driver inattention monitoring

Manuscript received February 13, 2019; revised September 19, 2019; accepted November 21, 2019. Date of publication December 10, 2019; date of current version February 2, 2021. This work is part of the research programme i-CAVE with project number 14893, which is partly financed by the Dutch Research Council (NWO). The Associate Editor for this article was S. A. Birrell. *(Corresponding author: Wouter S. Schinkel.)*

The authors are with the Department of Mechanical Engineering, Eindhoven University of Technology, Eindhoven, The Netherlands (e-mail: w.s.schinkel@tue.nl; t.p.j.v.d.sande@tue.nl; h.nijmeijer@tue.nl).

Digital Object Identifier 10.1109/TITS.2019.2956598

systems, including the most recent and futuristic technologies. A study considering a brought-in sensor is [14], which uses the front and rear camera of a smartphone to detect driver distraction or tiredness with machine learning and computer vision algorithms. In [15] a driver steering torque estimator has been used to detect human intervention torque. Driver intervention is detected if the estimated driver torque exceeds a certain threshold, simulation results show that intervention can be detected within 0.15 s. However, in the experiments a minimum intervention duration of 0.2 s has been considered for it to be a successful intervention, increasing the response time.

The response time of the intervention detection is an important aspect for driver safety. Driver safety applications such as ABS and ESC can have a response time of tenths of milliseconds [16]. However, in this case a driver is in the loop, who has slow dynamics compared to safety applications [17]. The human-machine interaction is a popular research topic because of the developments in (semi-) autonomous vehicles. One of the subtopics in this field is the time required for a driver to take over control of the vehicle after a take-over request, which is generally shortened to TOR. A good indicator for the average take-over time can be obtained from review articles [18], [19]. The authors of [18] have analyzed 25 different articles and found a take-over time of 2.47 s $\pm$ 1.42 s for the transition from automated to manual driving. However, because of the considerable variance in the results, the authors recommend to use the full range of take-over times (1.9 s to 25.7 s) rather than the mean or median. A meta-analysis of 129 studies has been presented in [19], where it is also stated that the results for take-over times vary strongly. A distribution of 520 mean take-over times reveals that all mean values are at least 0.5 s, with most values concentrated between 1 s and 4 s. It has to be noted that most studies regarding take-over times consider a fixed time budget, which refers to the timeframe a driver has to take over control. An example of such a study is [20], where time budgets of 2.5 s to 3.5 s have resulted in an average take-over time of 1.14 s. The authors of [21] showed that time budgets from 1.5 s to 2.8 s are sufficient for some drivers, but not all drivers are able to prevent accidents, implying the take-over time should be longer than 2.8 s to ensure accident prevention. Several studies have analyzed the take-over behavior in more detail [22]–[26], and the results can be used to define a lower limit for the response time. Results presented in [22], where a take-over time interval of 7 s has been used, show that after a take-over request from the vehicle the drivers need 0.70 s to 0.75 s (median) to touch the steering wheel, while actual steering inputs are given after 1.55 s to 1.60 s (median) respectively. This implies that after touching the steering wheel, drivers need approximately 0.85 s to apply an input. Similarly, comparing the median values presented in [23] gives at least 0.8 s between touching and moving the steering wheel. The results presented in [24] are in agreement with the aforementioned, giving in-between times varying from 0.65 s to 1.10 s. The authors of [25], who have considered non-critical transitions including putting away a tablet or phone, present take-over times for (un)monitored driving and having the eyes closed. Subtracting mean values implies that the drivers need 1.67 s to 4.61 s from moving the hands to taking over control. A significantly shorter time between touching the steering wheel and initiating a steering response has been presented in [26], where the mean value is 0.17 s.

Recent studies [4]–[15] for driver intervention detection show that detecting an intervention is realizable. Moreover, the technology is already available on commercial passenger vehicles [6], [13]. However, several drawbacks to these solutions can be identified. The most important drawbacks include the necessity for additional hardware, the high demand on the CPU load for data processing, the cost, susceptibility to environmental effects, and the need for driver inputs. Also, the studies are often limited to emergency/hazardous situations [20], [27], [28], vehicle initiated take-over requests [18], [19], [29], [30], or focused on driver state monitoring [6], [13], [31].

The goal of this article is to present and demonstrate a safe novel driver intervention detection method which does not suffer from the drawbacks mentioned above. This study is a proof of concept and in this study it is assumed that the driver would like to take over control in non-critical scenarios such as during discomfort or distrust in the control system, and that the hands of the driver are placed on the steering wheel when the driver performs an intervention. Safety related applications are out of the scope of this study. Also, the effect of different weather conditions is not taken into account. The basic concept is that a perturbation is applied to the steering system and driver intervention is detected based on the steering system response. To achieve this the steering system dynamics have been analyzed using the electric power steering (EPS) motor and steering column angle sensor. Driver intervention is detected by estimating the steering system dynamics, and from this estimate analyze whether the driver is in contact with the steering wheel [32]–[34]. This study is a continuation of work presented at the AVEC'18 [35]. The vehicle and steering system are modelled such that relevant dynamics can be simulated, and the model has been parametrized with frequency response measurements. Based on the observed steering system dynamics, an intervention detection algorithm has been developed. This algorithm is designed to be robust to disturbances and have a low computational load. Measurements with a test vehicle are in agreement with the simulation results.

This article is organized as follows. In section II the modeling and parametrization of the relevant vehicle dynamics is discussed. In section III the proposed driver intervention detection method is discussed with focus on the detection logic. In section IV the results are discussed, consisting of simulations and experiments. A discussion is presented in section V, including the limitations of the presented detection method and a comparison with existing solutions, followed by the conclusions presented in section VI.

II. System Model

The dynamics are described with a single-track vehicle model, connected to a two degree-of-freedom (DOF) steering system model. A Volkswagen Lupo 3L 2003 has been used

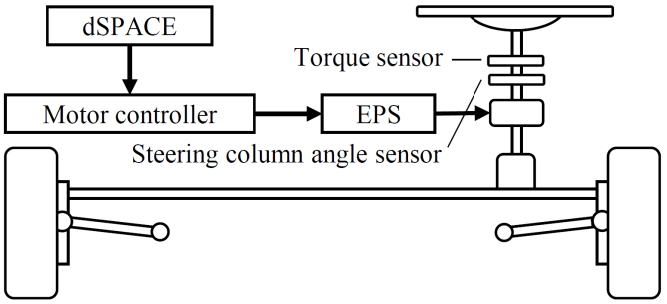

Fig. 1. Schematic drawing of the modified steering system of the Volkswagen Lupo 3L, indicating that the steering system can be controlled via a computer (dSPACE DS1103).

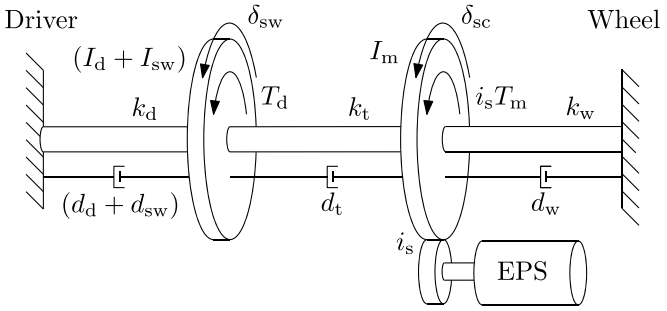

Fig. 2. Steering system model with two masses, one being the effective mass of the EPS motor, steering column, and wheel, and one being the effective mass of the steering wheel and driver.

as a test vehicle in this study, which is a compact passenger vehicle. The steering system of the test vehicle has been modified such that it can be controlled via a computer as shown in Fig. 1. For this study use has been made of the EPS motor torque and the steering column angle sensor. The steering system is equivalent to those in modern passenger vehicles, making the detection algorithm applicable to a wide range of vehicles.

A. Steering System Model

The steering system dynamics are modeled with a two DOF mass, spring, and damper system and the driver model presented in [36] is used. An illustration of this model is shown in Fig. 2. All model parameters are assumed to be constant. The steering system model, with steering column angle δ_{sc} and steering wheel angle δ_{sw} as DOF, results in the following equations of motion:

$$\begin{aligned} &I_m i_s^2 \ddot{\delta}_{sc} \\ &= -(d_t + d_w)\dot{\delta}_{sc} + d_t\dot{\delta}_{sw} - (k_t + k_w)\delta_{sc} + k_t\delta_{sw} + i_s T_m \quad (1) \\ &(I_d + I_{sw})\ddot{\delta}_{sw} \\ &= -(d_d + d_{sw} + d_t)\dot{\delta}_{sw} + d_t\dot{\delta}_{sc} - (k_d + k_t)\delta_{sw} + k_t\delta_{sc} + T_d \\ &\qquad (2) \end{aligned}$$

where the effective moment of inertia of the driver, steering wheel, and EPS motor is I_d, I_{sw}, and I_m. The latter also accounts for the influence of the steering column and wheels. The stiffness of the driver, torsion bar, and wheels, is k_d, k_t, and k_w. Jacking torques and the self-aligning moment are included in the effective road wheel stiffness k_w.

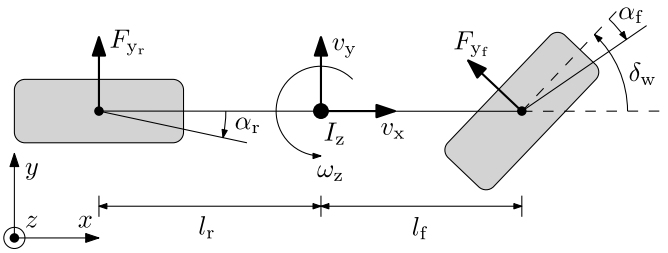

Fig. 3. Illustration of the single-track vehicle model.

The damping for the driver, steering wheel, torsion bar, and wheels is d_d, d_{sw}, d_t, and d_w respectively. The gear ratio between the steering column and the EPS motor is i_s. The model inputs are a driver torque T_d and an EPS motor torque T_m.

The steering system model has been used to simulate the steering system dynamics for both automated driving (no driver) and manual driving (driver included). When no driver is present or interacting with the steering wheel, all driver parameters are set to zero. Different drivers can be accounted for by tuning the driver parameters [24]. The influence of different drivers on the intervention detection is not investigated in this study.

B. Vehicle Model

The single-track vehicle model is widely used for the analysis of lateral vehicle dynamics. The longitudinal vehicle velocity is considered to be constant in this model, but the theory also holds for quasi-steady-state situations, such as a slow braking maneuver [37]. The model is depicted in Fig. 3 and has two DOF, the lateral vehicle velocity v_y, and the yaw rate ω_z. The longitudinal or forward vehicle velocity is v_x, and I_z is the moment of inertia around the z-axis. The lateral tyre forces are F_{y_f} and F_{y_r} for the front and rear axles. The tyre forces represent the sum of the left and right tyre on each axle. The side slip angles are α_f and α_r. The distance from the front and rear axle to the center of gravity is l_f and l_r. The input of the single-track model is the wheel angle δ_w, which is coupled with the steering system model via $\delta_{sc} = i_w\delta_w$ with i_w being a fixed gear ratio. The equations of motion of the single-track vehicle model are

$$m\dot{v}_y = -\frac{C_{\alpha_f} + C_{\alpha_r}}{v_x}v_y - \left(v_x + \frac{l_f C_{\alpha_f} - l_r C_{\alpha_r}}{v_x}\right)\omega_z + \frac{C_{\alpha_f}\delta_{sc}}{i_w}, \quad (3)$$

$$I_z\dot{\omega}_z = -\frac{l_f C_{\alpha_f} - l_r C_{\alpha_r}}{v_x}v_y - \frac{l_f^2 C_{\alpha_f} + l_r^2 C_{\alpha_r}}{v_x}\omega_z + \frac{l_f C_{\alpha_f}\delta_{sc}}{i_w}, \quad (4)$$

where m is the vehicle mass, and C_{α_f} and C_{α_r} are the cornering stiffness for the front and rear axles, and linear tyre characteristics are considered [37]. The complete model, consisting of the single track vehicle model and the steering system model, is described with (1), (2), (3), and (4).

C. Model Parametrization

The model has been validated and parametrized with frequency response measurements. The test vehicle is equipped with a dSPACE DS1103 system, operating at a sampling frequency of $f_s = 1$ kHz. A multi-sine torque has been applied

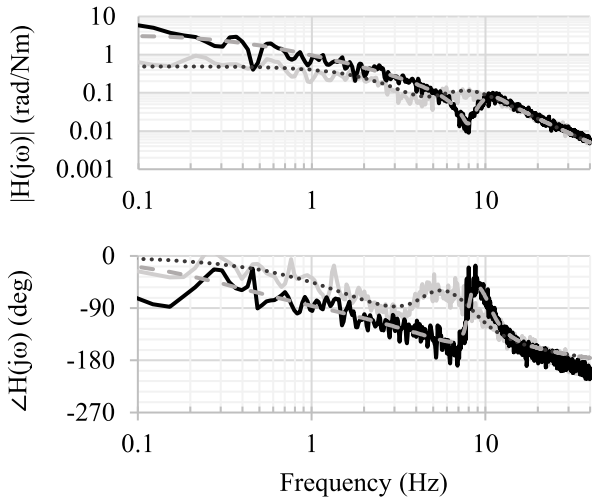

Fig. 4. Measured and parametrized frequency response between the EPS torque and steering column angle for both hands on the steering wheel and hands off the steering wheel. The measured response for hands on is (——), (‥‥) is the simulation for hands on, (▬) is the measurement for hands off, and (– –) is the simulation for hands off.

as input signal via the EPS motor with a frequency content ranging from 0.010 Hz to 40 Hz. Measurements with and without a driver have been performed, all with a longitudinal velocity of $v_{\mathrm{x}} = 0$ km/h with the vehicle placed on turning plates, which is a good representation of on-road driving [38]. Previous work shows that the influence of the longitudinal velocity is negligible in the frequency range of interest [38], and therefore this effect is not considered. The parametrization has been performed by fitting the transfer function from the EPS motor torque to the steering column angle

$$H_{T_{\mathrm{m}}\rightarrow\delta_{\mathrm{sc}}}(j\omega) = \frac{\mathcal{L}\{\delta_{\mathrm{sc}}\}(j\omega)}{\mathcal{L}\{T_{\mathrm{m}}\}(j\omega)} \tag{5}$$

on the frequency response measurements.

The measurements results are shown in Fig. 4 together with the parametrized model response. The vehicle and steering system parameters have been obtained using the measurement with no driver. The driver parameters have then been identified using the measurement with driver hands on the steering wheel. In the latter case the already identified vehicle parameters have been used. By solely adjusting the driver parameters, the dynamics with and without driver can be simulated. The measurement results reveal a significant difference in the steering column response for driver hands-on and driver hands-off. Most interesting is the shift of the anti-resonance frequency of the steering column. This effect is used in the detection logic, which is explained in the following section.

III. Intervention Detection Method

Driver intervention is detected by analyzing whether the driver is holding the steering wheel. By analyzing the differences in response for hands-on and hands-off the steering wheel, a notable distinction can be identified at 7.8 Hz (Fig. 4). For driver hands-off the steering wheel, the anti-resonance of the steering column is located at this frequency. Because the difference in transfer function gain $\left(\left|H_{T_{\mathrm{m}}\rightarrow\delta_{\mathrm{sc}}}(j\omega)\right|\right)$ at 7.8 Hz is substantial, it should be possible to detect this. The intervention detection method presented in this article estimates the transfer function gain at this specific frequency, which is then used to detect driver intervention.

A. Detection Logic

In order to make an estimate of the transfer function gain $\left|H_{T_{\mathrm{m}}\rightarrow\delta_{\mathrm{sc}}}(j\omega)\right|$, both the input T_{m} and output δ_{sc} need to be analyzed. A sinusoidal perturbation is applied to the steering system, which is described with

$$T_{\mathrm{dis}}(t) = A\sin(2\pi f_{\mathrm{d}} t), \tag{6}$$

where A is a constant amplitude and f_{d} the perturbation frequency. Choosing the perturbation frequency as $f_{\mathrm{d}} = 7.8$ Hz has multiple advantages. First, the transfer function gain $\left|H_{T_{\mathrm{m}}\rightarrow\delta_{\mathrm{sc}}}(j\omega)\right|$ for hands-on the steering wheel is roughly 7 times higher than for hands-off the steering wheel. Second, the yaw response and lateral vehicle velocity only show a limited response when the driver is not holding the steering wheel. Last, this frequency does not interfere with the frequency spectrum for regular driving, which is limited to frequencies up to 0.5 Hz [17]. However, one needs to be aware that the convergence speed of the intervention detection is related to the perturbation frequency, higher frequencies may result in a smaller response time, but can induce a notable yaw response.

1) Transfer Function Estimation: Now that the perturbation signal is defined, the transfer function gain can be estimated using the input signal $u = T_{\mathrm{m}}$ and the output signal $y = \delta_{\mathrm{sc}}$. A method for estimating this gain has been discussed in [39], which makes use of the auto- and cross-correlation and power- and cross-spectrum. The power-spectrum is also known as the auto-spectrum. The auto-correlation is defined as

$$r_{\mathrm{uu}}[l] = \lim_{N\rightarrow\infty}\frac{1}{2N+1}\sum_{i=-N}^{N} u[i]u[i+l], \tag{7}$$

where i is the sample number, l the sample delay and N a constant. From here onwards a discrete time notation is being used. Similarly, the cross-correlation is defined as

$$r_{\mathrm{uy}}[l] = \lim_{N\rightarrow\infty}\frac{1}{2N+1}\sum_{i=-N}^{N} u[i]y[i+l]. \tag{8}$$

Using the auto- and cross-correlation, the auto- and cross-spectrum can be computed. The power-spectrum is described as

$$\phi_{\mathrm{uu}}(\omega) = \sum_{l=-\infty}^{\infty} r_{\mathrm{uu}}[l]\, e^{-j\omega l}, \tag{9}$$

where ω is the frequency in rad/s and j is an imaginary number. The power-spectrum is independent of the sample delay l. The cross-spectrum is described as

$$\phi_{\mathrm{uy}}(\omega) = \sum_{l=-\infty}^{\infty} r_{\mathrm{uy}}[l]\, e^{-j\omega l}. \tag{10}$$

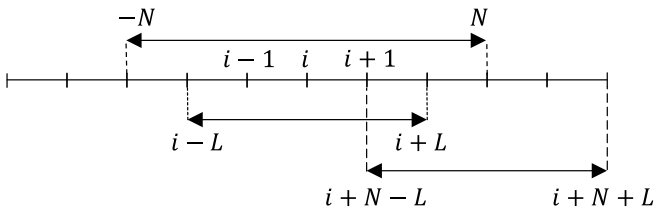

Fig. 5. Illustration of the required samples in order to compute the auto- and cross-correlation and power- and cross-spectrum, where i corresponds with the current sample.

With the above expressions the estimated transfer function gain can be calculated as

$$\left|\hat{H}_{T_{\mathrm{m}}\rightarrow\delta_{\mathrm{sc}}}(j\omega)\right| = \frac{\phi_{\mathrm{uy}}(\omega)}{\phi_{\mathrm{uu}}(\omega)}. \tag{11}$$

We now have an expression for the transfer function gain which can be evaluated at a selected frequency. Regarding the computational load of the detection logic this is favorable, since the estimate only has to be computed at the perturbation frequency, f_{d}. However, taking a closer look at (7), (8), (9), and (10), shows that both N and l go to infinity, meaning infinite samples are needed to compute these functions. Because the detection logic has to be implemented in a real-time application, estimates of (7), (8), (9), and (10) need to be obtained.

Introducing a finite value for N and considering

$$l \in \Lambda = \{-L, -L+1, -L+2, \ldots, L\} \tag{12}$$

with L a real finite constant, allows to make approximations of (7), (8), (9), and (10). The estimated cross-correlation can now be described with

$$\hat{r}_{\mathrm{uy}}[l, i-\tau] = \frac{1}{2N+1}\sum_{k=i-N}^{i+N} u[k]y[k+l], \quad l \in \Lambda. \tag{13}$$

In this equation a sample delay is introduced, being $\tau = N+L$. Replacing $y[k+l]$ with $u[k+l]$ in (13) gives the expression for the auto-correlation. From (13) it can be observed that in order to compute $\hat{r}_{\mathrm{uy}}[l, i-\tau]$, $N+l$ future samples must be considered. This effect is clarified with the illustration shown in Fig. 5. The need for future samples evidently results in a sample delay τ for real-time implementation. Similarly to the approximation for the cross-correlation, the cross-spectrum can be approximated as

$$\hat{\phi}_{\mathrm{uy}}(\omega)[l, i-\tau] = \hat{r}_{\mathrm{uy}}[l, i-\tau]\, e^{-j\omega l}, \quad l \in \Lambda. \tag{14}$$

The approximation for power-spectrum is obtained by replacing $\hat{r}_{\mathrm{uy}}[l, i-\tau]$ with $\hat{r}_{\mathrm{uu}}[l, i-\tau]$. Using the presented approximations, the following expression is obtained for the estimated transfer function gain:

$$\left|\hat{H}_{T_{\mathrm{m}}\rightarrow\delta_{\mathrm{sc}}}(j\omega)[i-\tau]\right| = \frac{\hat{\phi}_{\mathrm{uy}}(\omega)[i-\tau]}{\hat{\phi}_{\mathrm{uu}}(\omega)[i-\tau]}. \tag{15}$$

We can now make an estimate of $\left|H_{T_{\mathrm{m}}\rightarrow\delta_{\mathrm{sc}}}(j\omega)\right|$ at every sample, which can be used to detect whether the driver is in contact with the steering wheel. The next step is to make a translation from driver hands touching the steering wheel to driver intervention.

2) Detecting Driver Intervention: A driver touching the steering wheel is considered as a driver originated intervention. Whether the driver is touching the steering wheel, defined as h, is described with

$$h[i] = \begin{cases} 1 & \text{for } \left|\hat{H}_{T_{\mathrm{m}}\rightarrow\delta_{\mathrm{sc}}}(j\omega_{\mathrm{d}})[i]\right| > K \\ 0 & \text{for } \left|\hat{H}_{T_{\mathrm{m}}\rightarrow\delta_{\mathrm{sc}}}(j\omega_{\mathrm{d}})[i]\right| \leq K. \end{cases} \tag{16}$$

The signal equals 1 when driver hands are in contact with the steering wheel, which is true if the estimated gain exceeds a constant threshold K. The threshold K is extracted from the measurements in Fig. 4, and should always satisfy

$$\left|\hat{H}_{T_{\mathrm{m}}\rightarrow\delta_{\mathrm{sc}}}(j\omega_{\mathrm{d}})\right|_{\text{hands-off}} \leq K \leq \left|\hat{H}_{T_{\mathrm{m}}\rightarrow\delta_{\mathrm{sc}}}(j\omega_{\mathrm{d}})\right|_{\text{hands-on}}. \tag{17}$$

Note that the estimated transfer function gain is evaluated only at the perturbation frequency, $\omega_{\mathrm{d}} = 2\pi f_{\mathrm{d}}$.

Robustness to measurement noise and disturbances has to be realized to improve safety. Considering the last P samples, driver detection is only detected if all P samples show a positive detection for driver hands on the steering wheel. I.e.,

$$D[i] = \begin{cases} 1 & \text{for } \sum_{m=0}^{P-1} h[i-m] = P \\ 0 & \text{for } \sum_{m=0}^{P-1} h[i-m] < P, \end{cases} \tag{18}$$

where D is the detected driver intervention, which is equal to 1 for driver hands on the steering wheel. Since the last P samples are considered, implementing (18) evidently introduces a time delay of $\tau = (P-1)T_{\mathrm{s}}$, with T_{s} being the sampling time. This results in a trade-off between increased safety/robustness and additional time delay. The additional delay only affects the response time for the detection of hands on the steering wheel. Transitioning from hands on the steering wheel to hands off the steering wheel, only requires a single value of $h[i] = 0$ with $i \in \{-P+1, -P+2, \ldots, 0\}$.

3) Time Delays: Now that the core of the detection logic has been presented, we can take a closer look at the time delays introduced by approximating the correlation functions and auto- and cross-spectrum. The time delay introduced in (13) depends on N and L. In order to achieve a high convergence speed, both N and L need to be chosen as small as possible.

A lower bound for N is obtained by analyzing the relevant samples. Since we are only interested in estimating the transfer function gain at the perturbation frequency f_{d}, all relevant dynamics are solely located at this frequency. The lower bound for N can be limited to

$$N_{\mathrm{LB}} = \left\lceil \frac{1}{2 f_{\mathrm{d}} T_{\mathrm{s}}} \right\rceil, \tag{19}$$

which ensures that at least of full period of the perturbation signal is analyzed.

The sample delay l contains information about the phase between $u[i]$ and $y[i]$. The phase information from Fig. 4 is used to define a lower bound for L, resulting in

$$L_{\mathrm{LB}} = \left\lceil \frac{\angle H_{T_{\mathrm{m}}\rightarrow\delta_{\mathrm{sc}}}(j\omega_{\mathrm{d}})}{360 f_{\mathrm{d}} T_{\mathrm{s}}} \right\rceil, \tag{20}$$

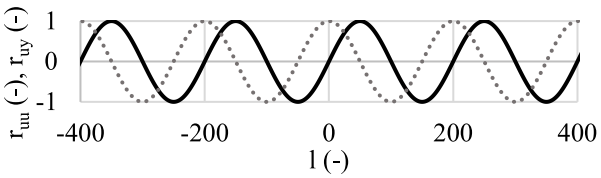

Fig. 6. The normalized auto-correlation (——) and cross-correlation (- - - -) functions for a sinusoidal input signal and delayed output signal, showing the periodicity of the correlation functions. The input-output delay is 50 samples.

where $\angle H_{T_m \to \delta_{sc}}(j\omega_d)$ is the phase delay in degrees. There are two options for selecting the phase delay, the phase for hands on the steering wheel and for hands off the steering wheel. One option is to select the largest of the two, ensuring that the relevant data is always included in the set ranging from sample $i - N_{LB} - \Lambda_{LB}$ to sample $i + N_{LB} + \Lambda_{LB}$. In this specific study, the phase delay at $f_d = 7.8$ Hz is the largest for hands off the steering wheel and will be considered to determine Λ_{LB}.

4) Reducing the Computational Load: The set of samples which is used in the estimation can be reduced, because the phase delay of the system is known a priori via system identification. The set Λ to can be reduced to a sub-set $\Lambda_s \subset \Lambda$. For a sine wave signal with constant frequency f, the auto-correlation shows a peak at $l = [n/(2T_s f)]$ with $n \in Z^{\geq}$. This effect is illustrated in Fig. 6. The location of the peaks allows to reduce the set Λ for the auto-correlation to $l \in \Lambda_{s,uu} = \{0; 0 \subset \Lambda\}$. If the output signal is simply a delayed version of the input signal, the cross-correlation peaks at $= [n/(2T_s f) + l_d]$ as shown in Fig. 6, where l_d is the sample delay from input to output. Because the steering controller does not actuate frequencies above 0.5 Hz during normal operation [17], it is assumed that the perturbation signal is the only signal influencing the cross-correlation at this frequency, neglecting the effect of noise and disturbances. Using the phase from Fig. 4, the set Λ considered for the cross-correlation is reduced to $l \in \Lambda_{s,uy} = \{l_{\text{hands on}}, l_{\text{hands off}}; l_{\text{hands on}}, l_{\text{hands off}} \subset \Lambda\}$. Here $l_{\text{hands on}}$ and $l_{\text{hands off}}$ are the phase at $f_d = 7.8$ Hz for driver hands on the steering wheel and driver hands off the steering wheel. By including both $l_{\text{hands on}}$ and $l_{\text{hands off}}$, no distinction has to be made between the scenarios of having driver hands (not) in contact with the steering wheel. In order to ensure an equal number of samples is used in the computation of the auto- and cross-correlation, $\Lambda_{s,uu}$ is increased to $\Lambda_{s,uu} = \{0, 0; 0 \subset \Lambda\}$.

B. Performance Criteria

To analyze the performance of the detection logic, several criteria are defined. A straightforward criterion is the value of the estimated transfer function gain. Theoretically this value should converge to the actual frequency response. However, the approximations made in the foregoing might influence the extent to which this is possible.

Next is the response time or convergence speed of the detection logic. The information on take-over times presented in Section I is used to define an upper bound for the response time of the intervention detection algorithm. From the articles discussed above the minimum mean take-over time is at least 0.50 s. The in-between time for touching and moving the steering wheel is generally 0.65 s or longer, with the exception of one study presenting an in-between time of 0.17 s [22]–[26]. We aim to achieve a response time of 0.65 s maximum, $t_r \leq 0.65$ s, since we consider non-critical intervention scenarios and do not consider safety related applications.

Finally, the number of false-positives and false-negatives should be as small as possible. One should prevent a false-positive detection, such that the control system cannot be shut down while the driver is not interacting with the vehicle.

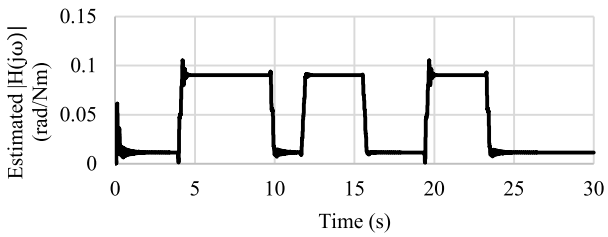

Fig. 7. Estimated transfer function gain, where the steering system response is simulated using the parametrized model from (1), (2), (3), and (4).

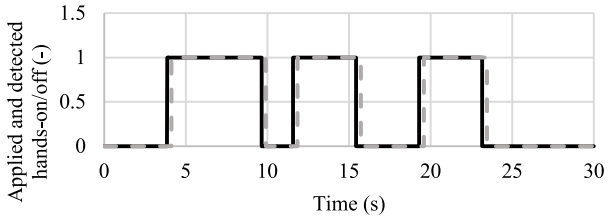

Fig. 8. Applied (——) and detected (- - - -) hands on the steering wheel and hands off the steering wheel. These results are obtained by simulating the steering system response using (1), (2), (3), and (4).

IV. Results

The results are divided into four parts: 1) a simulation study; 2) a verification with on-road measurements; 3) an analysis of the response time; and 4) a true-false detection analysis. In all simulations the effect of measurement noise and road disturbances has been neglected. The parameters of the intervention detection algorithm have been chosen identical for the simulations and measurements, such that a fair comparison can be made ($N = 128, l_{\text{hands on}} = 39, l_{\text{hands off}} = 30, P = 128, K = 0.025$).

A. Simulation Study

A simulation study has been performed using the system model described with (1), (2), (3), and (4). Driver intervention has been simulated by switching between the identified driver parameters and no driver ($I_d, d_d, k_d = 0$). The estimated transfer function gain is shown in Fig. 7 and the detected driver intervention in Fig. 8. The estimated values from Fig. 7 approach the measurements from Fig. 4, and Fig. 8 shows that all interventions are detected. The detection logic does have a small delay as discussed in section III.A. When switching from hands on to hands off and vice versa, oscillations are introduced by the sudden in/exclusion of stiffness, mass, and damping, which might result in additional delays in the intervention detection.

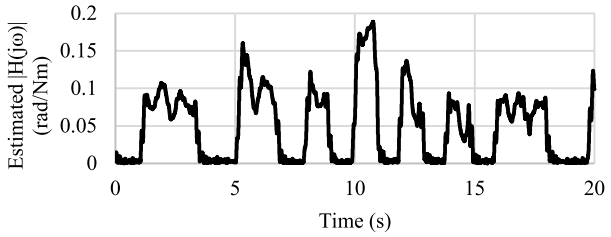

Fig. 9. Estimated transfer function gain from on-road measurements. In this case the vehicle was driving on a straight asphalt road with no speed bumps and potholes.

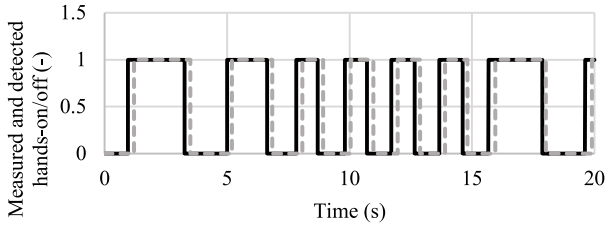

Fig. 10. Applied (▬) and detected (- - -) hands on the steering wheel and hands off the steering wheel. The results are obtained driving on a straight asphalt road with no speed bumps and potholes.

B. On-road Measurements

The on-road measurement have been performed on two types of roads, asphalt and Belgian cobblestones. The asphalt road is a high quality straight road with no speed bumps. The cobblestone road is slightly curved, includes large potholes, and is of lower quality compared to the asphalt road, this road can be considered as an extreme example. During experiments it has been discovered that the sensor resolution of the steering column angle is a limiting factor for the detection method, motions within the sensor resolution resulted in an inaccurate estimation of the transfer function gain. Therefore, the disturbance torque amplitude has been chosen such that the sensor resolution does not affect the detection algorithm. Whether the driver is in contact with the steering wheel has been measured via a pressure sensor placed on the steering wheel rim, this signal has been used as a ground truth to calculate the response time of the intervention detection.

1) Asphalt: The estimated transfer function gain for driving on the asphalt road is shown in Fig. 9 and the applied and detected driver intervention are both shown in Fig. 10. The estimated transfer function gain has a higher variance compared to the simulation results, caused by measurement noise, road disturbances and driver inputs. However, there is still a significant difference in estimated transfer function gain for the scenario with and without a driver. The detected driver intervention from Fig. 10 confirms that the presented detection logic is robust to noise and disturbances from driving on a smooth asphalt road. With the given test set-up the level of disturbances coming from the road cannot be determined. The response time of the detection logic is similar to what is found via simulations, roughly 0.3 s for the detection of hands on and hands off the steering wheel, and all interventions are detected.

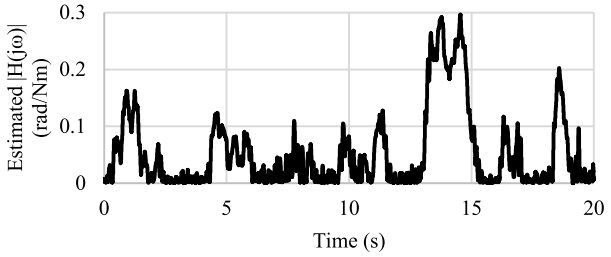

Fig. 11. Estimated transfer function gain from on-road measurements. In this case the vehicle was driving on a cobblestone road with large potholes.

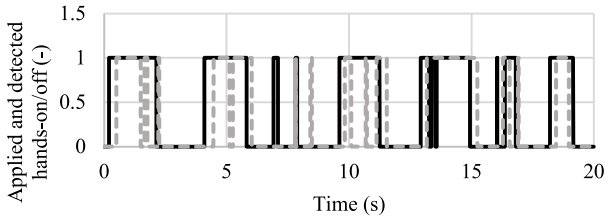

Fig. 12. Applied (▬) and detected (- - -) hands on the steering wheel and hands off the steering wheel. The results are obtained driving on a cobblestone road with large potholes.

2) Belgian Cobblestones: The results for driving on a cobblestone road are shown in Fig. 11 and Fig. 12. The estimated transfer function gain in Fig. 11 shows significant differences compared to the results for driving on an asphalt road, illustrating the effect of larger road disturbances. The increase in disturbances has been confirmed with a PSD analysis, which shows an increased level of noise for all frequencies, reducing the ratio between the estimated transfer function gain for hands-on/off. The intervention detection is inconsistent with false detections every now and then. However, the majority of the false detections are false-negatives and there is a minimal amount of false-positive detections, the latter is far worse in terms of driver safety. By comparing the results from the cobblestone road to the asphalt road, it is found that the performance of the detection algorithm depends on the road quality and is positively correlated with the road quality.

C. Response Time Analysis

The response time for driver intervention detection has been analyzed by performing over 200 take-over procedures in simulation and experiments. The experiment has been executed with the vehicle placed on turning plates, thus having a velocity of 0 km/h.

The results are listed in Table I, which reveal that the average response time for the detection of hands-on the steering wheel and hands-off the steering wheel is similar for the simulation and measurements. However, for the measurements, the maximum response time as well as the standard deviation is higher in comparison to the simulation results, which is not surprising considering the simulations did not include noise and disturbances. A response time of $t_r \leq 0.65$ s is successfully achieved, making the intervention detection suitable for the majority of the interventions [22]–[26]. With the implementation of (18) it is expected that the response time for the detection of hands on the steering wheel is lower compared to hands off the steering wheel, but results show that this is not the case. The threshold K has been chosen

TABLE I

RESPONSE TIME OF THE DETECTION LOGIC, OBTAINED FROM OVER 200 DRIVER INTERVENTIONS

	Average response time (s)	Standard deviation (s)	Maximum response time (s)
Simulation; Hands-on	0.274	0.0142	0.293
Simulation; Hands-off	0.280	0.0108	0.292
Measurement; Hands-on	0.300	0.0265	0.375
Measurement; Hands-off	0.295	0.0301	0.385

TABLE II

CONDITIONS FOR A TP, TN, FP, AND FN WITH APPLIED HOO BEING APPLIED HANDS-ON/OFF BY THE DRIVER AND DETECTED HOO BEING THE OUTPUT OF THE INTERVENTION DETECTION ALGORITHM

	Condition
TP	max(Applied HOO $([t - t_r, t])$) = 1 & Detected HOO (t) = 1
TN	min(Applied HOO $([t - t_r, t])$) = 0 & Detected HOO (t) = 0
FP	max(Applied HOO $([t - t_r, t])$) = 0 & Detected HOO (t) = 1
FN	min(Applied HOO $([t - t_r, t])$) = 1 & Detected HOO (t) = 0

relatively low, resulting in an increased response time for the detection of hands on and a decreased response time for the detection of hands off, explaining the marginal differences in response time.

D. True-false detection analysis

For a more extensive performance analysis the detection behavior in terms of true positives (TPs), true negatives (TNs), false positives (FPs), and false negatives (FNs) has been analyzed. Because the detection algorithm has a time delay, it is only fair to take this into account in the false-positive analysis. An intervention detection is labeled as TP if the driver hands are placed on the steering wheel in the interval $[t - t_r, t]$ where t_r is the assumed response time of the detection algorithm, thus taking previous samples into account. The classification conditions that are used in this analysis are listed in Table II.

The performance in terms of true and false detections is shown in Fig. 13 for an assumed response time of 0 s and 0.385 s (matching the maximum from Table I) and in Fig. 14 for response times ranging from 0 s to 5 s, both figures include the asphalt and cobblestone road measurements results. Fig. 13 shows that driving on an asphalt road resulted in 7.6 % FPs and 9.8 % FNs with the assumed response time set to 0 s. Increasing the assumed response time to 0.385 s reduced the FPs and FNs both to 0.0 %, a result that is confirmed with Fig. 14. Assuming a response time of approximately 0.3 s, matching the average values from Table I, results in 0 % FPs and FNs for the measurements on asphalt. The results indicate that a lower road quality negatively influences the number of FPs and FNs. Fig. 13 shows that the number of FPs for the cobblestone road is similar to the results for the asphalt road. In terms of safety this is a satisfying results, since a false positive means that

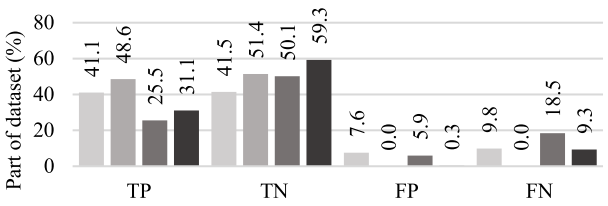

Fig. 13. Performance in terms of TPs, TNs, FPs, and FNs for; asphalt with $t_r = 0$ s (▭), asphalt with $t_r = 0.385$ s (▭), cobblestones with $t_r = 0$ s (▭), and cobblestones with $t_r = 0.385$ s (▭), all expressed as a percentage of the total number of samples in the dataset.

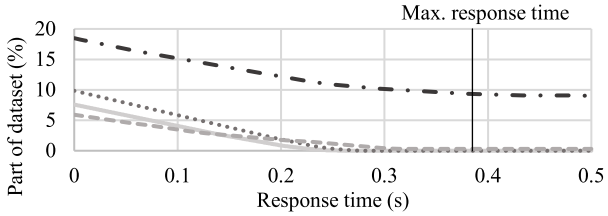

Fig. 14. The FPs and FNs as a function of the response time taken into account in the analysis with (——) the FPs for asphalt, (·····) the FNs for asphalt, (– – –) the FPs for cobblestones, and (— · —) the FNs for cobblestones.

the driver is not holding the steering wheel, but the algorithm estimated that the steering wheel is being held. In case of a FP, control can be shifted to the driver, who is at that time not in contact with the steering wheel, thus creating a very unsafe situation. The number for FNs does show a large increase when driving on a cobblestone road compared to an asphalt road. Fig. 14 shows that the number of FPs and FNs converges around $t_r = 0.3$ to 0.4 s, after which only the FNs for cobblestone roads show a value not close to zero.

V. DISCUSSION

The results show that the presented intervention detection method can be used to detect driver intervention with an average response time of 0.3 s and maximum of 0.4 s, meeting our aim of 0.65 s. However, in order to reach $t_r \leq 0.17$ s, matching the lowest in-between time obtained from literature, the response time should be decreased. The response time can potentially be reduced by perturbing the steering system at a higher frequency. At the same time however, not actuating on the anti-resonance of the road wheel angle will result in a larger yaw response. To avoid this one can change the steering system for one with a higher anti-resonance of the road wheel angle such that the yaw response is kept to a minimum whilst maintaining a significant difference in transfer function gain for hands-on/off. It is not expected that only increasing the perturbation frequency can reduce the response time enough the meet safety requirements. In order to further reduce the response time, additional research is required.

Measurements results show successful detection of driver intervention via the proposed algorithm and thus without additional hardware. However, it has to be noted that the algorithm does not necessarily outperform existing solutions which do require additional hardware. A pressure sensor, which has been used as a reference for hands-on/off in this study, has a significantly smaller response time. Other existing solutions may also outperform the presented detection method in other

TABLE III
PERFORMANCE OF THE PRESENTED DETECTION ALGORITHM IN COMPARISON TO EXISTING SOLUTIONS

Study	Category	Performance in comparison to study
[4]	Vision	Shorter response time and less false detections
[5]	Vision	Similar in terms of true and false detections
[8]	Biometric	Less false detections
[10]	Wearable	Similar to better in terms of true and false detections, shorter response time
[14]	Brought-in	Less false detections
[15]	Other	Similar to shorter response time without requiring steering inputs

aspects, such as robustness for lower quality roads and external disturbances. The presented algorithm can be used alongside other methods to increase the performance and robustness. The goal of this study is to present and demonstrate a novel driver intervention detection method which does not require additional, which is successfully achieved. The presented method solely uses in-vehicle sensors, the steering angle and steering torque sensor, to detect driver intervention. Furthermore, the drawbacks of existing solutions are also eliminated. No significant increase in computational load has been found after including the detection algorithm. The marginal effect on the CPU load of the operation system is as expected, considering the low complexity of the equations. It may be noted that high CPU loads are mainly present in vision systems, which require image processing of one or multiple image recordings. Some existing solutions are susceptible to environmental effects such as rapid variations in light intensity. Although this system is not influenced by light intensity, the effect of disturbances from the road do affect the system performance, which is shown by the differences between driving on asphalt and cobblestone roads. For future work it is recommended to improve the robustness to external disturbances, such that the performance on lower quality roads is similar to the performance on higher quality roads. Because the presented detection algorithm does not require additional hardware and uses on-board sensor information which is already available, the system can easily be implemented into the control system of a vehicle. This algorithm does require information of the steering system dynamics, which can be obtained via system identification. However, for the application of mass production vehicles, these dynamics are already known, resulting in low costs for implementation onto new vehicles. Finally, the detection algorithm does not require any driver input to detect an intervention.

Comparing the performance with existing solution shows that the presented detection algorithm generally performs similar or better in areas the systems can be compared. Table III shows the differences in performance for a number of studies. One has be aware that it is difficult to make a full and thus fair comparison, since not all studies include the same performance metrics as used in this study. Also, most studies use a lab set-up, which evidently has less disturbances than a test vehicle driving on a (poor) road.

Limitations of the presented detection algorithm include the road quality, the considered intervention scenario and the steering angle sensor resolution. In this study it is assumed that whenever the driver performs an intervention, the steering wheel is touched. However, this might not be true for all interventions, since a driver can also perform an intervention without touching the steering wheel. For this reason the presented approach is limited to situations where a driver does touch the steering wheel. Also, non-critical interventions are considered, this method is not yet suitable for safety applications. Finally, the amplitude of the disturbance torque has a lower bound directly related to steering angle sensor resolution, higher resolution sensors can decrease this amplitude and therefore also decrease the induced yaw response.

VI. CONCLUSION

Driver intervention detection via on-line transfer function estimation is successfully realized without using additional hardware. The algorithm for driver intervention detection presented in this article can be implemented in nearly all modern passenger vehicles. The method has been validated with measurements, whose results are in agreement with the simulation results. Via measurements it has been found that the performance of the driver intervention detection depends on the road quality. More specifically, the performance is positively correlated to the road quality. The number false-negative detections increases for lower quality roads, while the number of false-positives seems to be unaffected by the road quality. A response time analysis shows that using the presented detection method, driver intervention is successfully detected within the desired timeframe. The detection algorithm does not suffer from the same drawbacks as existing solutions but still has a similar or better performance. However, limiting factors and areas of future research are identified, being the reduction of the response time of the system, the performance and robustness on low quality roads, the effect of the steering column angle sensor resolution, and the considered intervention scenario.

REFERENCES

[1] *Surface Vehicle Recommended Practice: Taxonomy and Definitions for Terms Related to Driving Automation Systems for On-Road Motor Vehicles*, SAE International Standard J3016, Jun. 2018.

[2] D. Gibson. (Jan. 2017). Cruise control and adaptive cruise control: The complete guide. Auto Express, London, U.K. Accessed: Oct. 21, 2017. [Online]. Available: https://www.autoexpress.co.uk/car-tech/98225/cruise-control-and-adaptive-cruise-control-the-complete-guide

[3] T. Litman, "Generated traffic and induced travel: Implications for transport planning," Victoria Transp. Policy Inst., Victoria, BC, Canada, Tech. Rep., Aug. 2016. Accessed: Sep. 18, 2018 [Online]. Available: https://www.vtpi.org/gentraf.pdf

[4] C. Tran and M. M. Trivedi, "Driver assistance for 'keeping hands on the wheel and eyes on the road,'" in *Proc. IEEE-ICVES*, Pune, India, Nov. 2009, pp. 97–101.

[5] T. H. N. Le, Y. Zheng, C. Zhu, K. Luu, and M. Savvides, "Multiple scale faster-RCNN approach to driver's cell-phone usage and hands on steering wheel detection," in *Proc. IEEE Conf. CVPRW*, Las Vegas, NV, USA, Jun. 2016, pp. 46–53.

[6] S. Kaplan, M. A. Guvensan, A. G. Yavuz, and Y. Karalurt, "Driver behavior analysis for safe driving: A survey," *IEEE Trans. Intell. Transp. Syst.*, vol. 16, no. 6, pp. 3017–3032, Dec. 2015, doi: 10.1109/TITS.2015.2462084.

[7] C. Qian, X. Sun, Y. Wei, X. Tang, and J. Sun, "Realtime and robust hand tracking from depth," in *Proc. IEEE Conf. CVPR*, Columbus, OH, USA, Jun. 2014, pp. 1106–1113.

[8] S. Mühlbacher-Karrer *et al.*, "A driver state detection system—Combining a capacitive hand detection sensor with physiological sensors," *IEEE Trans. Instrum. Meas.*, vol. 66, no. 4, pp. 624–636, Apr. 2017, doi: 10.1109/TIM.2016.2640458.

[9] H. Silva, A. Lourenço, and A. Fred, "In-vehicle driver recognition based on hand ECG signals," in *Proc. ACM Int. Conf. IUI*, Lisbon, Portugal, Feb. 2012, pp. 25–28.

[10] C. Bi, J. Huang, G. Xing, L. Jiang, X. Liu, and M. Chen, "Safe-Watch: A wearable hand motion tracking system for improving driving safety," in *Proc. IEEE/ACM 2nd Int. Conf. IoTDI*, Pittsburgh, PA, USA, Jun. 2017, pp. 223–232.

[11] C. Karatas *et al.*, "Leveraging wearables for steering and driver tracking," in *Proc. IEEE INFOCOM*, San Francisco, CA, USA, Apr. 2016, pp. 1–9.

[12] B.-G. Lee and W.-Y. Chung, "Wearable glove-type driver stress detection using a motion sensor," *IEEE Trans. Intell. Transp. Syst.*, vol. 18, no. 7, pp. 1835–1844, Jul. 2017, doi: 10.1109/TITS.2016.2617881.

[13] V. Melnicuk, S. Birrell, E. Crundall, and P. Jennings, "Towards hybrid driver state monitoring: Review, future perspectives and the role of consumer electronics," in *Proc. IEEE Intell. Vehicles Symp. (IV)*, Gothenburg, Sweden, Aug. 2016, pp. 1392–1397.

[14] C.-W. You *et al.*, "CarSafe App: Alerting drowsy and distracted drivers using dual cameras on smartphones," in *Proc. 11th Annu. Int. Conf. Mobile Syst., Appl., Services (MobiSys)*, Taipei, Taiwan, 2013, pp. 13–26.

[15] X. Wang, L. Guo, and Y. Jia, "Online sensing of human steering intervention torque for autonomous driving actuation systems," *IEEE Sensors J.*, vol. 18, no. 8, pp. 3444–3453, Apr. 2018, doi: 10.1109/JSEN.2018.2805381.

[16] R. Ranjith and R. Shanmughasundaram, "Simulation of safety critical applications for automotive using multicore scheduling," in *Proc. ICCI-CCT*, Kumaracoil, India, Dec. 2016, pp. 12–16.

[17] J. Ackermann, "Robust decoupling, ideal steering dynamics and yaw stabilization of 4WS cars," *Automatica*, vol. 30, no. 11, pp. 1761–1768, Nov. 1994, doi: 10.1016/0005-1098(94)90079-5.

[18] A. Eriksson and N. A. Stanton, "Takeover time in highly automated vehicles: Noncritical transitions to and from manual control," *Hum. Factors*, vol. 59, no. 4, pp. 689–705, Jun. 2017, doi: 10.1177/0018720816685832.

[19] B. Zhang, J. de Winter, S. Varotto, R. Happee, and M. Martens, "Determinants of take-over time from automated driving: A meta-analysis of 129 studies," *Transp. Res. F, Traffic Psychol. Behav.*, vol. 64, pp. 285–307, Jul. 2019, doi: 10.1016/j.trf.2019.04.020.

[20] K. Zeeb, A. Buchner, and M. Schrauf, "What determines the take-over time? An integrated model approach of driver take-over after automated driving," *Accident Anal. Prevention*, vol. 78, pp. 212–221, May 2015, doi: 10.1016/j.aap.2015.02.023.

[21] A. P. van den Beukel and M. C. van der Voort, "The influence of time-criticality on Situation Awareness when retrieving human control after automated driving," in *Proc. ITSC*, The Hague, The Netherlands, Oct. 2013, pp. 2000–2005.

[22] P. Kerschbaum, K. Omozik, P. Wagner, S. Levin, J. Hermsdörfer, and K. Bengler, "How does a symmetrical steering wheel transformation influence the take-over process?" in *Proc. Hum. Factors Ergonom. Soc. Eur. Chapter Annu. Conf.*, Prague, Czech Republic, Oct. 2016, pp. 95–106.

[23] P. Kerschbaum, L. Lorenz, and K. Bengler, "A transforming steering wheel for highly automated cars," in *Proc. IEEE Intell. Vehicles Symp. (IV)*, Seoul, South Korea, Jun. 2015, pp. 1287–1292.

[24] B. Zhang, E. S. Wilschut, D. M. C. Willemsen, and M. H. Martens, "Transitions to manual control from highly automated driving in non-critical truck platooning scenarios," *Transp. Res. F, Traffic Psychol. Behav.*, vol. 64, pp. 84–97, Jul. 2019, doi: 10.1016/j.trf.2019.04.006.

[25] C. Gold, D. Damböck, L. Lorenz, and K. Bengler, "'Take over!' How long does it take to get the driver back into the loop?" in *Proc. Hum. Factors Ergonom. Soc. Annu. Meeting*, Sep. 2013, pp. 1938–1942.

[26] S. Petermeijer, P. Bazilinskyy, K. Bengler, and J. de Winter, "Take-over again: Investigating multimodal and directional TORs to get the driver back into the loop," *Appl. Ergonom.*, vol. 62, pp. 204–215, Jul. 2017, doi: 10.1016/j.apergo.2017.02.023.

[27] R. Happee, C. Gold, J. Radlmayr, S. Hergeth, and K. Bengler, "Take-over performance in evasive manoeuvres," *Accident Anal. Prevention*, vol. 106, pp. 211–222, Sep. 2017, 10.1016/j.aap.2017.04.017.

[28] I. Politis, S. Brewster, and F. Pollick, "Using multimodal displays to signify critical handovers of control to distracted autonomous car drivers," *Int. J. Mobile Hum. Comput. Interact.*, vol. 9, no. 3, pp. 1–16, Jul. 2017, doi: 10.4018/ijmhci.2017070101.

[29] A. P. van den Beukel, M. C. van der Voort, and A. O. Eger, "Supporting the changing driver's task: Exploration of interface designs for supervision and intervention in automated driving," *Transp. Res. F, Traffic Psychol. Behav.*, vol. 43, pp. 279–301, Nov. 2016, doi: 10.1016/j.trf.2016.09.009.

[30] S. M. Petermeijer, S. Cieler, and J. C. F. de Winter, "Comparing spatially static and dynamic vibrotactile take-over requests in the driver seat," *Accident Anal. Prevention*, vol. 99, pp. 218–227, Feb. 2017, doi: 10.1016/j.aap.2016.12.001.

[31] Y. Dong, Z. Hu, K. Uchimura, and N. Murayama, "Driver inattention monitoring system for intelligent vehicles: A review," *IEEE Trans. Intell. Transp. Syst.*, vol. 12, no. 2, pp. 596–614, Jun. 2011, doi: 10.1109/TITS.2010.2092770.

[32] J.-W. Lee, Y. H. Lee, and B. B. Litkouhi, "Driver hands on/off detection during automated lane centering/changing maneuver," U.S. Patent 2010/0 228 417 A1, Mar. 6, 2010.

[33] J. A. Urhahne, "Hands-on-off steering wheel detection for motor vehicle," U.S. Patent 9 096 262 B2, Mar. 13, 2013.

[34] S. Trimboli and R. Hause, "Method and system for detecting steering wheel contact," U.S. Patent 2014/0 371 989 A1, Jun. 12, 2014.

[35] W. S. Schinkel, T. P. J. van der Sande, and H. Nijmeijer, "Driver intervention detection in automated vehicles," presented at the AVEC, 2018.

[36] A. Pick and D. Cole, "Neuromuscular dynamics and the vehicle steering task," in *Proc. 18th IAVSD Symp.*, Kanagawa, Japan, Aug. 2003, pp. 182–191.

[37] H. B. Pacejka, "Tyre characteristics and vehicle handling and stability," in *Tyre and Vehicle Dynamics*, 2nd ed. Oxford, U.K.: Butterworth-Heinemann, 2006, ch. 1, pp. 1–60.

[38] J. Loof, "Modeling and control of a truck steering-system for active driver support," Ph.D. dissertation, Dept. Mech. Eng., Eindhoven Univ. Technol., Eindhoven, The Netherlands, Feb. 2018.

[39] K. J. Keesman, "Correlation methods," in *System Identification: An Introduction*. London, U.K.: Springer, 2011, ch. 4, pp. 43–58.

Wouter S. Schinkel was born in 1992. He received the M.Sc. degree in mechanical engineering from the Delft University of Technology in 2016. He is currently pursuing the Ph.D. degree with the Eindhoven University of Technology.

His research interests include cooperative and automated driving with focus on vehicle state estimation and vehicle dynamics control.

Tom P. J. van der Sande was born in 1986. He received the M.Sc. degree in automotive technology and the Ph.D. degree in mechanical engineering from the Eindhoven University of Technology in 2011 and 2015, respectively.

He is currently a Researcher with the Dynamics and Control Group, Eindhoven University of Technology. His past research involved the control of vehicle dynamics using by-wire features, such as active suspension and steer-by-wire. His current research focus is in the field of cooperative and automated driving with a strong focus into the practical application of both.

Henk Nijmeijer (F'00) was born in 1955. He is a Full Professor with the Eindhoven University of Technology, Eindhoven, The Netherlands, where he is also the Chair of the Dynamics and Control Group. He has authored a large number of journal and conference papers, and several books, and is or was at the editorial board of numerous journals.

Mr. Nijmeijer is an Editor of *Communications in Nonlinear Science and Numerical Simulations*. He is appointed Honorary Knight of the "Golden Feedback Loop" (Norwegian University of Science and Technology) in 2011. Since 2011, he has been an IFAC Council Member. In 2015, he was the Scientific Director of the Dutch Institute of Systems and Control, Delft, The Netherlands. He is a Program Leader of the Dutch research program "Integrated Cooperative Automated Vehicles." Since 2017, he has been the Director of the Graduate Program Automotive Technology, Eindhoven University of Technology. He was a recipient of the 1990 IEE Heaviside premium and the 2015 IEEE Control Systems Technology Award.